Wavefront decomposition and propagation through complex models with analytical ray theory and signal processing

Paul Cristini, Eric de Bazelaire

Journal of Computational Acoustics

Wavefront decomposition and propagation through complex models with analytical ray theory and signal processing

P. CRISTINI
CNRS-UMR5212
Laboratoire de Modélisation et d'Imagerie en Géosciences de Pau
Université de Pau et des Pays de l'Adour
BP 1155, 64013 Pau Cedex, France
paul.cristini@univ-pau.fr

E. De BAZELAIRE
11, Route du bourg
64230 Beyrie-en-Béarn, France
eric.debazelaire@wanadoo.fr

Received (Day Month Year)
Revised (Day Month Year)

We present a novel method which can perform the fast computation of the times of arrival of seismic waves which propagate between a source and an array of receivers in a stratified medium. This method combines signal processing concepts for the approximation of interfaces and wavefronts, and ray theory for the propagation of wavefronts. This new approach leads to the redefinition and simplification of the model through which waves propagate. The modifications are governed by the spectral characteristics of the source signal. All rays are computed without any omission at a much lower cost in computing time than classical methods.

Keywords: wavefront decomposition; ray tracing; reflection; transmission; circular interface; caustic.

1. Introduction

Ray tracing is commonly used for the calculation of traveltimes and amplitudes of seismic events. Many algorithms have been developped (see Ref. 1 for a comprehensive review on ray methods) which all have their advantages and drawbacks. Nevertheless they all provide poor results when the geometry of the interfaces is complex. Classical ray tracing techniques are unstable in such contexts, which leads to difficulties in finding the eigenrays which connect the source to the receivers. Some rays are not found, which can make the interpretation of complex tectonics dangerously complicated. Similarly, classical numerical methods provide unsatisfactory results because of the smoothing of the velocity model they require.[2] The complex geometry of interfaces is generally associated with strong impedance contrasts which are not well modelled with a smoothed model. Finally, even if ray methods are much faster than the numerical solution of the wave equation, they are not fast enough for 3D inversion. The design of a very fast and comprehensive ray tracing algorithm is still of critical importance.

More generally, direct calculations of wave propagation problems are the basis of inverse procedures which aim at recovering predetermined parameters. These parameters are in general relevant to the physics of the problem that is to be solved and may provide the requested information needed for the answer to a specific question. There is a common feeling shared by people working in the field of inverse problems that only a small part of the amount of information which is calculated is really used to recover these abovementioned parameters. Consequently a natural question that arises after these remarks is : How can we reduce the amount of computation for solving the direct problem of wave propagation, in such a way that, in order to solve a given inverse problem, we calculate only what is necessary ? For example, in geophysics, the determination of traveltime maps is often the preliminary step required before performing the inversion process and only the times of arrival of the different waves are used, whereas all the other details of the structure of the received signal are not taken into account. The purpose of this paper is to give an answer to such a question in the context of the evaluation of the times of arrivals of acoustic waves which propagate through a complex velocity model.

We start with the remark that the computations which are performed have to be measured and the traveltimes have to be evaluated from these measurements. This evaluation is not an error free process. It is both limited by the resolving power Δt_R of the source signal and by the time sampling interval τ. The resolving power indicates the size of the smallest detail the signal can "see" (resolution), while the time sampling interval provides the accuracy of the measurement of the position of a detected detail (precision). Consequently, the computation should be in adequation with the precision and the resolution of the source signal in order to avoid unnecessary computational effort. For instance, an error can be tolerated in the evaluation of traveltimes if it is controlled and if it is less than $\tau/2$. Because of the limitation due the sampling of the signal, there is no need to achieve better accuracy. The objective of this paper is to show how it is possible to simplify the problem of reflection/ transmission of waves at interfaces whose geometry is complex using the possibility of making errors in the evaluation of traveltimes. For the sake of simplicity, we consider that the surrounding media are homogeneous but extensions to more complex media can be easily done. It results in the design of a novel method entitled Signal Based Ray Tracing (SBRT) which is the subject of this paper. This topic was already tackled in Refs. 3 and 4 but not with the approach proposed here. Contrary to the abovementioned works, we pay careful attention to the justification of all the concepts used to elaborate the proposed method. In this way, we gain an insight into the behaviour of SBRT. Moreover, the methodology proposed in Refs. 3 and 4 was only approximate contrary to the work presented in this paper.

This paper is organized as follows. In Sec. 2, we explain how we simplify the velocity model through which the waves propagate, taking into account the spectral bandwidth of the source signal. This leads to the interpolation of the interfaces of the model with error control with circular arcs. Then, we introduce the concept of Point Source Beam (PSB) which is the basis of the decomposition of wavefronts into elements whose propagation is more simple to handle, and which takes advantage of the decomposition of interfaces into simple elements. Since this decomposition is approximate, we give an evaluation of the error committed when using it. The fourth section is devoted to the control of this error in the context of the reflection or refraction of acoustic waves at a circular interface. We investigate in details the evaluation of this error to give an insight into its physical meaning. We show how to adapt the decomposition by adding new PSB to the wavefront representation when it is necessary (i.e., when the error exceeds half the time sampling interval of the signal). Finally, we give an example of the use of this decomposition for the determination of the times of arrivals in the context of seismic wave propagation over a salt dome.

2. Simplification of the model with circle arc interpolation

The starting point of our method originates from the observation that the tool used to probe an acoustic or elastic medium is not perfect. It is a broadband wave which has its own resolving power. As a consequence, uncertainties are inherent in the process of determining the times of arrival. It is not possible and not necessary to determine the exact traveltime along a ray with such a signal. As a result, the time accuracy which is obtained from numerical models is often much higher than what can be obtained from measurements. The same results could be obtained with less computational effort. The first step of Signal Based Ray tracing (SBRT) is to simplify the velocity model through which waves propagate according to the resolving power of the source signal.

2.1. *Resolving power of the source signal*

Wave propagation can be studied within the framework of information theory where the ray which connects the source to the receiver is, by analogy, the transmission channel whose capacity depends on the spectral characteristics of the source signal. For the sake of simplicity, we consider noiseless channels and therefore rather refer to the work of Gabor[5] instead of that of Shannon.[6]

Now, let us enonciate some remarks. A signal can be characterized in the time-frequency plane by its time-bandwidth product $T_d \times B_d$, where T_d is the duration of the signal and B_d is the bandwidth of the signal. A property of this product is that it is lower bounded :

$$T_d \times B_d = N \geq 1$$

N represents the number of signals which can be separated within the time duration T_d. It is a measure of the *information richness* of the signal.[7] This relation is known as the Heisenberg-Gabor inequality. It illustrates the fact that a signal cannot have simultaneously an arbitrary small support in time and in frequency. The lower bound is reached for gaussian signals. As a consequence, the resolving power Δt_R of a signal is given by :

$$\Delta t_R = 1/B_d$$

This property is analogue to the Rayleigh criterion[8] used in optics. It means that if the traveltime difference between two events is less than this value, the signal only exhibits one peak. There are some details of the geometry of the interfaces that cannot be detected with the source signal which is used. This fact is not always taken into account in the construction of the model and its structure is often too complex. In order to take into account this fact, we need to modify the interfaces in such a way that the details that are undetectable are smoothed. It results in a model which is compatible with the resolving power of the source signal.

2.2. *Velocity model interpolation*

The choice of the type of interpolation is made with the objective of simplifying the wave propagation problem. We choose circle arcs with continuous first order derivative. This type of approximation is not common in the context of wave propagation studies, but is well-known in engineering design. The reason is the capability of the milling machines to move along straight lines and circular paths. As a consequence, a lot of attention has been paid to the possibility of interpolating a curve with circle arcs. Biarcs approximation, which has been developped for almost thirty years, is the procedure which is the most relevant to our needs. We used the ideas developped for computer numerical controllers in the context of reflection and transmission of seismic waves. We will emphasize on some specific points that arise in wave propagation. For more details on biarcs and their applications the reader can refer to several articles[9,10,11,12] which can be considered as entry points to the topic.

Approximation to data by C^1 arcs is of critical importance since we want to ensure the continuity of the reflection-refraction law. This type of continuity ensures the continuity of the normals along the arcs which approximate the interface. A biarc is a curve that connects two end-points smoothly with two circular arcs and matches the tangential directions at the connection points. We have to define some particular points where the G^1 continuity is not required. These points correspond to the presence of a fault for instance.

The approximation is realized in the following way. A first step consists in digitizing several points which are supposed to represent the interface to be approximated. A spline interpolation is then done to visualize the "real" interface and to check if the result of the interpolation corresponds to what the user wanted to get. Once this step is realized, the biarc approximation is performed following the different steps given in Ref. 9.

The key factor is the tolerance band, i.e. the quality of the approximation. It is given by :

$$\Delta e = c_0 \, \Delta t_R = \frac{c_0}{B_d} \tag{1}$$

where c_0 is a reference velocity and B_d the bandwidth of the source signal.

The number of biarcs used to approximate a given curve is growing as the tolerance factor is diminishing. In the geophysical context the tolerance is not the same below and up the curve because the velocities are different. Nevertheless, for practical reasons, we used the same tolerance for all interfaces, but it is possible to work with asymmetric tolerance bands, as indicated in Refs. 9 and 12. The value of the tolerance is calculated with c_0 as the lowest velocity present in the model. The influence of this choice is negligible on the

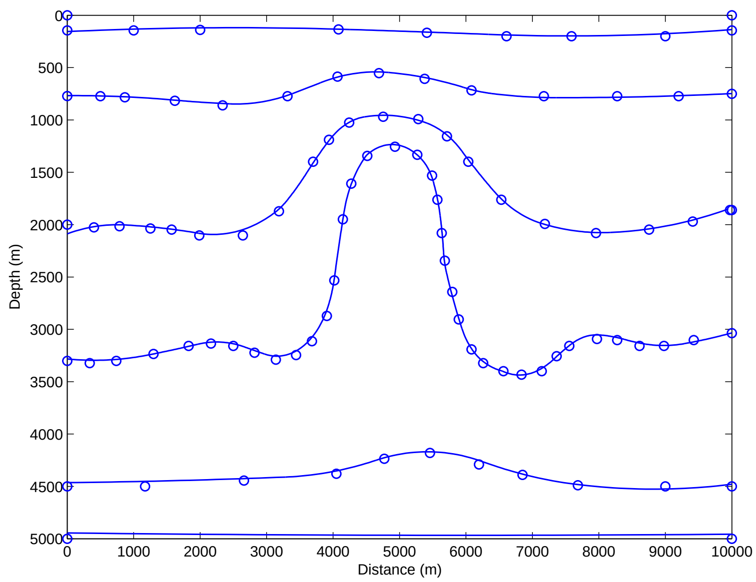

Fig. 1. Circle arc approximation of a salt dome model

number of biarcs necessary to construct the interfaces of the model.

An example of the results provided by the procedure we described in this section is shown in Fig. 1. The value of the tolerance is $\Delta e = 30m$ with a seismic bandwidth $B_d = 50Hz$ and a reference velocity $c_0 = 1500m.s^{-1}$. It can be seen that the circle arc approximation provides a very good interpolation of the original data.

3. Point Source Beam (PSB) approximation of wavefronts

The circle arc interpolation of the interfaces is the preliminary step of SBRT. It provides a new simplified model that can be used to calculate the propagation of rays. In order to give the basic principles of the method, we will only consider here constant velocity media. In this case, rays are straight lines and are easily calculated. Note that more complex media can be handled by the proposed method, but for the sake of simplicity, we will restrict to simple models here.

3.1. *Point Source Beam definition and implementation*

One characteristic of SBRT is that it deals with point source beams (PSB) instead of individual rays. This is a consequence of the possibility of making errors in the evaluation of the traveltimes. A PSB is defined by the following set :

$$B : \{\mathbf{S}, t, \theta_l, \theta_r\}$$

where $\mathbf{S}$ is the position of the source, t is a reference time associated to the source $\mathbf{S}$, θ_l and θ_r two angles with the horizontal direction. These two angles define the two extremal

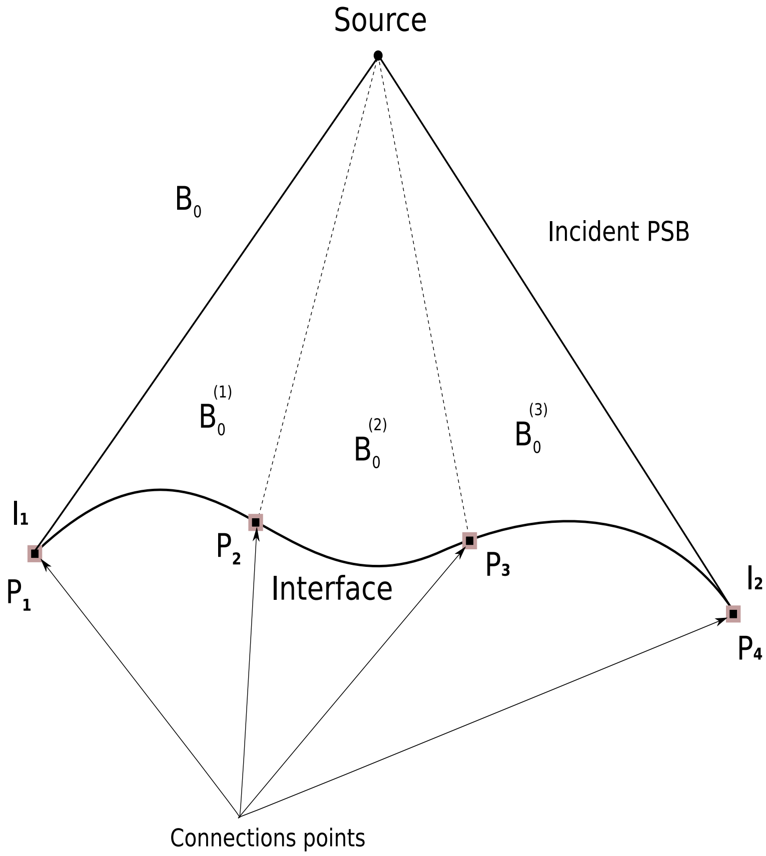

Fig. 2. Initial decomposition of an incident PSB . The interface is represented by three circle arcs.

rays of the beam. $\Theta = \theta_r - \theta_l$ is called the beam aperture.

An initial PSB associated with the set B_0 : $\{\mathbf{S_0}, t_0, \theta_l, \theta_r\}$ is considered. This PSB illuminates an interface with $(\mathbf{I_1}, \mathbf{I_2})$ as intersection points for the two extremal rays (see Fig. 2). As a result of the interpolation process described in the last section, several circle arcs constitute the portion of the interface located between $\mathbf{I_1}$ and $\mathbf{I_2}$. Let $\{\mathbf{P_i},\ i = 1,..,N\}$ be the set of connection points for these circle arcs. A first step of SBRT consists in dividing B_0 into several other PSB $B_0^{(i)}$ corresponding to all the circle arcs which constitute the portion of the interface which is illuminated by the initial PSB. Figure 2 illustrates this procedure. B_0 is now the juxtaposition of all PSB $B_0^{(i)}$:

$$B_0 = \bigcup_i B_0^{(i)} \;\; i = 0,..,N$$

where $B_0^{(i)}$: $\{\mathbf{S_0}, t_0, \theta_i, \theta_{i+1}\}$ with $\theta_0 = \theta_l$ and $\theta_N = \theta_r$

In addition to the abovementioned connection points, we have to consider points of the interface which correspond to rays which are tangent to the interface, or which corresponds to rays impinging at a critical angle which can also limit the extension of the PSB. Note that rays which reach the limits of the bounding box of the model are rejected.

After reflection or refraction, each PSB is transformed into another PSB associated with the set:

$$B_1^{(i)} : \{\mathbf{S_i}, t_i, \theta_i^{(1)}, \theta_{i+1}^{(1)}\}$$

The elements $\theta_i^{(1)}$ and $\theta_{i+1}^{(1)}$ of the set of the outgoing beam B_1 are easily determined by means of Snell's law. The element $\mathbf{S_i}$ is the intersection of the two rays associated with the previous angles. The only element which cannot be expressed directly is t_i since there are two paths which connect $\mathbf{S_0}$ to $\mathbf{S_i}$. Consequently, the association of a traveltime to $\mathbf{S_i}$ leads to an error if the path chosen is not the correct one. This is precisely this error which has to be controlled. It must not be greater than half the time sampling interval of the signal, otherwise the PSB $B_1^{(i)}$ has to be divided into as many PSB $B_1^{(k)}$ as necessary, such that :

$$B_1^{(i)} = \bigcup_k B_1^{(k)} \;\; k = 0, .., N$$

where $B_1^{(k)} : \{\mathbf{S_k}, t_k, \theta_k, \theta_{k+1}\}$ with $\theta_0 = \theta_i^{(1)}$ and $\theta_N = \theta_{i+1}^{(1)}$

In this way, each outgoing PSB is a "good" approximation of the outgoing wavefront. Consequently, SBRT acts as an interpolation process of the wavefront with circular arcs (constant curvature elements). The process is repeated with the successive interfaces which can be encountered until a criterion is fullfilled, i.e. when the PSB reaches the receivers or the bounding box of the model. In this way, the problem of the propagation of a wavefront through several interfaces is decomposed into a series of elementary problems which consist in solving the reflection or refraction of a point source beam at a circular interface. Since each elementary problem can be solved analytically (see Sec. 4), the speed of the computations is greatly improved in comparison to standard numerical tecnhiques.

3.2. *Error estimate of PSB approximation*

The reason why the reflection or refraction of a PSB is not a PSB lies in the fact that the centers of curvature associated with each ray belonging to the PSB move along a curve called caustic. In general, this curve does not degenerate to a point. Consequently, as indicated in Fig. 3, the approximation of a portion of the outgoing wavefront acts as a sampling of the caustic curve. We do not commit an error only in the traveltime evaluation, but also in the curvature evaluation, and these two errors are not independent. We propose here to evaluate these errors.

We begin with the evaluation of the traveltime in the context of the approximation of a wavefront by a PSB. If t_{J-1} denotes the time associated with the source of the incident PSB, then the time t_J associated with the source of the outgoing PSB is given by the following relation :

$$t_J = t_{J-1} + t_c \tag{2}$$

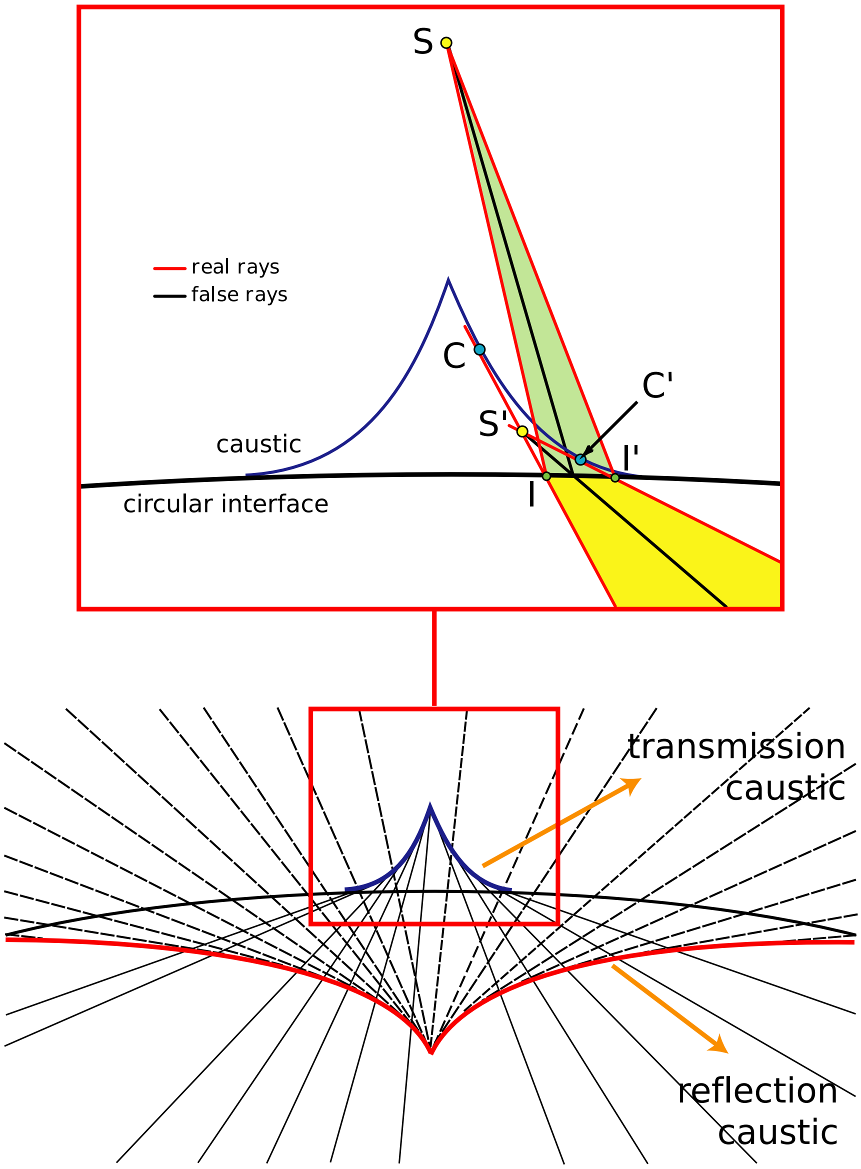

Fig. 3. PSB decomposition after reflection or refraction at a circular interface. The top figure indicates the geometry for the case of refraction. The bottom figure illustrates the decomposition of a PSB. The dashed lines represent the reflected rays and the full lines represent the refracted rays.

where t_c belongs to the following interval :

$$t_c \in \left[\frac{\overline{\mathbf{SI}}}{V_1} + \frac{\overline{\mathbf{IS'}}}{V_2}, \frac{\overline{\mathbf{SI'}}}{V_1} + \frac{\overline{\mathbf{I'S'}}}{V_2}\right] \qquad (3)$$

$\overline{\mathbf{SI}}$ and all other distances denote oriented segments between two points. The left bound denoted by T_1 and the right bound denoted by T_2 correspond to the two traveltimes calculated along the two extremal rays of the PSB. The value of t_c must be chosen within this interval. We choose $t_c = T_1$, the maximum error ΔT is therefore :

$$\Delta T = T_2 - T_1$$

As indicated previously, the approximation of the outgoing beam by a PSB corresponds to the approximation of a portion of the wavefront by a circle, i.e. by a constant curvature element. Therefore, the associated error in curvature can be calculated since the new point source which is chosen is the new local center of curvature. The error in curvature evaluation ΔG is simply given by :

$$\Delta G = \max\left\{|\overline{\mathbf{IS'}} - \overline{\mathbf{IC'}}|, |\overline{\mathbf{I'S'}} - \overline{\mathbf{IC}}|\right\} \tag{4}$$

where the points $\mathbf{C}$ and $\mathbf{C}'$ are determined by means of Fermat's principle extended to the second order (see the next section).

Once the expression of the error ΔT is obtained, the next step of SBRT consists in controlling this error. Each time the wavefront encounters an interface, an error is made and it adds to the previously made errors. It is a cumulative process. As a consequence, the error ϵ associated with an individual interface must take into account the number of interfaces likely to be encountered before attaining the receivers. It is given by :

$$\epsilon = \frac{\tau}{2(2N_i - 1)}$$

where N_i is the number of interfaces of the model and τ the time sampling interval. Note that this value is a maximum since the errors associated with each interface are not always of the same sign. We could have used the central limit theorem to evaluate the cumulative error, but the number of interfaces encountered is not always high enough to apply it.

The control of the error made after crossing each interface is then performed by solving the following equation :

$$|\Delta T(\mathbf{A})| = \epsilon \tag{5}$$

where the unknown $\mathbf{A}$ represents a point on the circle arc situated between $\mathbf{I}$ and $\mathbf{I}'$.

If this equation has no solution, then the outgoing PSB is a "good" approximation, otherwise it is necessary to divide it into two parts. One part corresponds to the arc IA which is "good" by definition. The other part AI' has to be tested in the same way as the original outgoing PSB. The process is repeated until all outgoing PSB are "good" approximations.

4. Solution to the PSB decomposition problem after Reflection/Transmission at a circular interface

The aim of this section is to give explicit expressions of the equations obtained in the previous section when the interface is circular. In a first part, we consider the reflection/transmission of an individual ray by means of Fermat's principle of traveltime stationarity extended to higher orders. This approach corresponds to a local point of view of the propagation process which enligths some specific points of SBRT. Then, in a second part, we return to the PSB decomposition problem by giving an explicit expression of Eq. (5) and by solving it.

Before starting the analysis, we give a description of the geometry of the problem and the sign conventions which are used. The geometry of the PSB decomposition problem at a circular interface is indicated in Fig. 4. An incident PSB $B_0 : \{\mathbf{S_0} : \{X_s, Y_s\}, t_0, \theta_l, \theta_r\}$ intersects a circular interface at the points $\mathbf{I}$ and $\mathbf{I}'$, the two intersection points associated with the two extremal rays of B_0. By considering the angular parametrization of the circle with an angle θ, the coordinates of these two points can be written as :

$$\mathbf{I} : \{X_c + R\cos\theta,\, Y_c + R\sin\theta\} \quad \mathbf{I}' : \{X_c + R\cos(\theta + \Delta\theta),\, Y_c + R\sin(\theta + \Delta\theta)\}$$

where X_c and Y_c are the coordinates of the point $\mathbf{C_0}$ the center of the circular interface and R is the radius of the circular interface.

We denote by i_1 and i_2 the angles of incidence of respectively the incident ray and the outgoing ray which intersect at point $\mathbf{I}$. These angles are counted counter-clockwise. We also use the sign convention of optics in order to characterize some distances. These quantities will be referred to as signed distances, with the convention that they are positive if they are oriented in the direction of propagation. This convention is used to ensure that the sign of the cosinus of the angle of incidence is always positive.

4.1. *Local analysis of ray propagation (Fermat's principle)*

The reflection/transmission of a ray at an interface is governed by Fermat's principle. Fermat's principle states that the path followed by a ray to connect a source to another point is the path for which the time taken has a stationnary value with respect to an infinitesimal variation. The traveltime T between points $\mathbf{S_0}$ and $\mathbf{O}$, a point belonging to the trajectory of the outgoing ray, is :

$$T = \frac{\overline{\mathbf{S_0I}}}{V_1} + \frac{\overline{\mathbf{IO}}}{V_2} = -\frac{L_1}{V_1} + \frac{L_2}{V_2} \tag{6}$$

where V_1 and V_2 are respectively the wave velocities in the incident medium and in the outgoing medium, and L_1 and L_2 are the signed distances respectively associated with $\overline{\mathbf{S_0I}}$ and $\overline{\mathbf{IO}}$. The expression of L_1 is :

$$L_1 = \pm\sqrt{(X - R\cos\theta)^2 + (Y - R\sin\theta)^2} \tag{7}$$

where $X = X_s - X_c$ and $Y = Y_s - Y_c$.

Since the circular interface can be parametrized as a function of the angle θ, an infinitesimal variation of the path corresponds to a derivation with respect to θ.

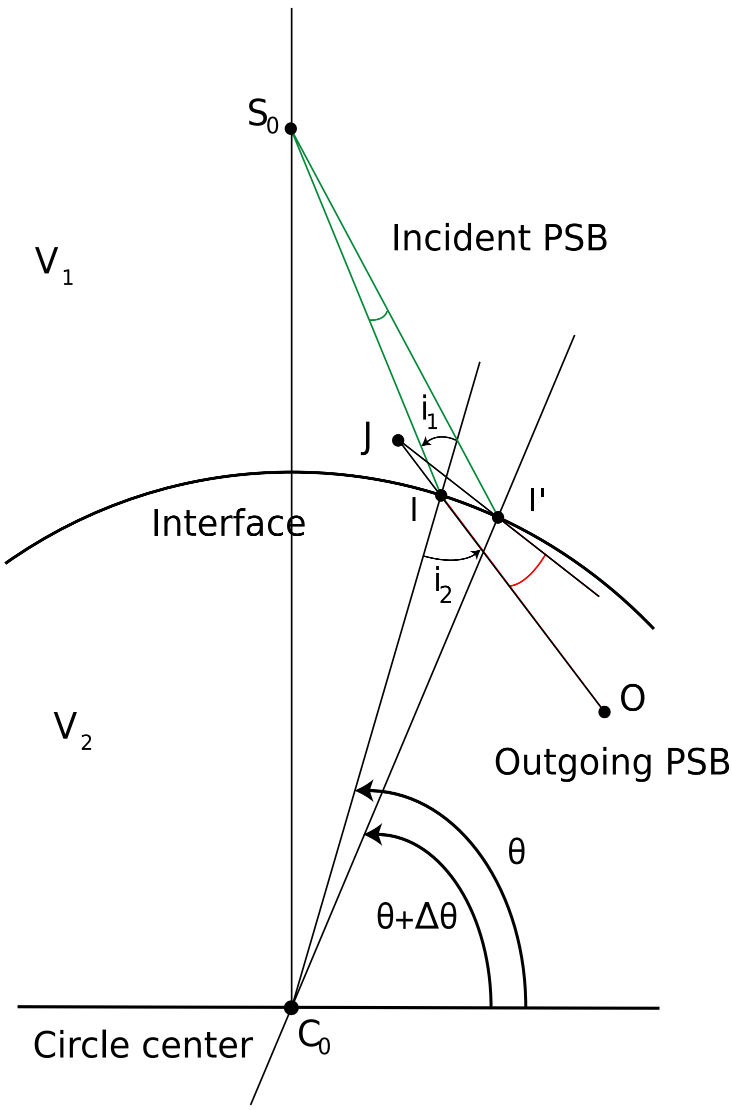

Fig. 4. Geometry of the propagation of a ray striking a circular interface

4.1.1. *First-order stationarity*

According to Eq. (7), the first-order derivative of L_1 with respect to θ is :

$$\frac{dL_1}{d\theta} = \frac{1}{2}\frac{2R\sin\theta\,(X - R\cos\theta) - 2R\cos\theta\,(Y - R\sin\theta)}{L_1} = \frac{R\,(X\sin\theta - Y\cos\theta)}{L_1} \tag{8}$$

By using Eq. (A.4), we have :

$$\frac{dL_1}{d\theta} = R_1\,\sin i_1 \tag{9}$$

In the same way, we get :

$$\frac{dL_2}{d\theta} = R_2 \sin i_2 \tag{10}$$

where R_1 and R_2 are the signed radii of the circular interface respectively associated with the incident ray and with the outgoing ray.

After Eq. (6), the first order derivative of traveltime with respect to θ is :

$$\frac{dT(\theta)}{d\theta} = \frac{R_1 \sin i_1}{V_1} - \frac{R_2 \sin i_2}{V_2}$$

Consequently the first order stationarity of traveltime leads to the well-known Snell's law :

$$\frac{R_1 \sin i_1}{V_1} = \frac{R_2 \sin i_2}{V_2} \tag{11}$$

This equality defines a new parameter which will be denoted by α. It is not common to express Snell's law in this form. The reason for this is the sign convention we use. The change of direction of the reflected ray is taken into account with the change of sign of either R_1 or R_2, instead of considering a negative wave velocity as usually done. For a given direction of the incident ray, Snell's law indicates the direction of the outgoing ray. In the case of reflection, we have, $V_1 = V_2$ and $R_1 = -R_2$.

4.1.2. *Second-order stationarity*

In order to obtain the second-order derivative of T with respect to θ, we need to evaluate the first-order derivative of angle i_1 with respect to θ. This quantity is obtained by derivating Eq. (A.4) and using Eq. (A.3). Some straightforward calculations lead to :

$$\frac{di_1}{d\theta} = \frac{R_1}{L_1} \cos i_1 - 1 \tag{12}$$

The same type of equation can be obtained for medium 2 and the second-order derivative of traveltime T with respect to θ is then given by :

$$\begin{aligned}\frac{d^2T(\theta)}{d\theta^2} &= \frac{d}{d\theta}\left(\frac{R_1 \sin i_1}{V_1} - \frac{R_2 \sin i_2}{V_2}\right) \\ &= R_1 \frac{\cos i_1}{V_1}\frac{di_1}{d\theta} - R_2 \frac{\cos i_2}{V_2}\frac{di_2}{d\theta} \\ &= R_1 \frac{\cos i_1}{V_1}\left(1 - \frac{R}{L_1}\cos i_1\right) - R_2 \frac{\cos i_2}{V_2}\left(1 - \frac{R}{L_2}\cos i_2\right)\end{aligned}$$

The nullification of the second order leads to the following equation which reduces to the thin lens formula of optics in the paraxial regime ($\cos i_1 \approx \cos i_2 \approx 1$) :

$$\frac{R_1}{V_1}\left(\cos i_1 - \frac{R_1}{L_1}\cos^2 i_1\right) = \frac{R_2}{V_2}\left(\cos i_2 - \frac{R_2}{L_2}\cos^2 i_2\right) \tag{13}$$

This equality defines a new parameter denoted by β. Equation (13) gives the location of the local center of curvature of the outgoing wavefront, i.e. the value of L_2. The points $\mathbf{C}$ or $\mathbf{C}'$ of Eq. (4) are determined from this equation. They can be either real or virtual, depending on the sign of L_2. If the angle of incidence of the ray is modified, then the new point source position moves to another location. The curve which corresponds to the locus of the successive centers of curvature is called caustic. The outgoing wavefront is circular only if the caustic reduces to a point, i.e. when stationarity to the third-order occurs, which is not the case in general.

4.1.3. *Third-order stationarity*

In the same way, it is straightforward to get for the third-order derivative of traveltime T with respect to θ:

$$\begin{aligned}\frac{d^3T(\theta)}{d\theta^3} = & R\frac{\sin i_1}{V_1}\left(1-3\frac{R}{L_1}\cos i_1\left(1-\frac{R}{L_1}\cos i_1\right)\right)\\ & -R\frac{\sin i_2}{V_2}\left(1-3\frac{R}{L_2}\cos i_2\left(1-\frac{R}{L_2}\cos i_2\right)\right)\end{aligned}$$

This equation is simplified by considering the two constants α and β introduced previously :

$$\frac{d^3T(\theta)}{d\theta^3} = 3R\alpha\beta\left(\frac{V_1}{L_1}-\frac{V_2}{L_2}\right) \tag{14}$$

It is then easy to see that the nullification of the third-order derivative only occurs in particular configurations. Stationarity beyond all orders requires that one of the following equations is verified :

$$\begin{aligned}\alpha &= 0\\ \beta &= 0\\ \left(\frac{V_1}{L_1}-\frac{V_2}{L_2}\right) &= 0\end{aligned}$$

The last equation is a special case in which the point $\mathbf{S}$ and the center of curvature of the outgoing wavefront are called Weierstrass points[8]. The caustic only reduces to a point in these specific configurations. In these cases, the reflection or refraction of a PSB is exactly another PSB.

4.2. *Traveltime difference evaluation*

Instead of working with infinitesimal variation of the position of a point on the interface, we consider the whole PSB. The variation of the distance between the point source $\mathbf{S_0}$ and the two points $\mathbf{I}$ and $\mathbf{I}'$ is $\Delta L_1 = L_1 - L_1'$ where L_1' is the signed distance associated with $\overline{\mathbf{I'S}}$ given by :

$$L_1' = \pm\sqrt{\left(R\cos\left(\theta+\Delta\theta\right)-X_s\right)^2+\left(R\sin\left(\theta+\Delta\theta\right)-Y_s\right)^2}$$

The square of this distance is :

$$L_1'^2 = R^2 + X^2 + Y^2 - 2R\left[X\cos(\theta+\Delta\theta) + Y\sin(\theta+\Delta\theta)\right]$$

Combining Eqs. (A.3) and (A.4), we get :

$$X\cos(\theta+\Delta\theta) + Y\sin(\theta+\Delta\theta) = R\cos\Delta\theta - L_1\cos(i_1+\Delta\theta)$$

As a consequence, we have :

$$\begin{aligned} L_1'^2 &= R^2 + X^2 + Y^2 - 2R\left[R\cos\Delta\theta - L_1\cos(i_1+\Delta\theta)\right] \\ L_1^2 &= R^2 + X^2 + Y^2 - 2R\left[R - L_1\cos i_1\right] \end{aligned}$$

Evaluating the difference of the two previous equations leads to the solution of the following second-order equation :

$$(\Delta L_1)^2 + 2L_1\Delta L_1 - 2R\left[R(1-\cos\Delta\theta) + L_1(\cos(i_1+\Delta\theta) - \cos i_1)\right] = 0$$

The root which is of interest is the one which tends to zero as $\Delta\theta$ tends to zero. It is defined by :

$$\Delta L_1(\Delta(\theta)) = -L_1 + sgn(L_1)L_1\sqrt{1 + \frac{2R}{L_1}(\cos(i_1+\Delta\theta) - \cos i_1) + \frac{2R^2}{L_1^2}(1-\cos\Delta\theta)} \quad (19)$$

which expresses the traveltime difference in the incident medium. The traveltime difference in the outgoing medium requires the determination of the intersection point **J** of the two extremal rays of the outgoing PSB. The directions of these two rays are determined from the angle of incidence i_2 in the following way :

$$\alpha = \theta + i_2 \qquad \alpha' = \theta + \Delta\theta + i_2'$$

After some straightforward calculations, the distance l between the points **I** and **J** and the distance l' between the points **I**$'$ and **J** can be expressed as :

$$\begin{aligned} l &= 2R\sin\left(\frac{\Delta\theta}{2}\right)\frac{\cos\left(\frac{\Delta\theta}{2} + i_2'\right)}{\sin(i_2 - i_2' - \Delta\theta)} \\ l' &= 2R\sin\left(\frac{\Delta\theta}{2}\right)\frac{\cos\left(\frac{\Delta\theta}{2} + i_2\right)}{\sin(i_2 - i_2' - \Delta\theta)} \end{aligned}$$

The traveltime difference is then given by :

$$l - l' = \frac{4R\sin\left(\frac{\Delta\theta}{2}\right)}{\sin(i_2 - i_2' - \Delta\theta)}\,\sin\left(\frac{i_2 - i_2' - \Delta\theta}{2}\right)\sin\left(\frac{i_2 + i_2'}{2}\right)$$

Or, after some manipulations, by :

$$l - l' = 2R\sin\left(\frac{\Delta\theta}{2}\right)\sqrt{\frac{1-\cos(i_2+i_2')}{1+\cos(i_2-i_2'-\Delta\theta)}}$$

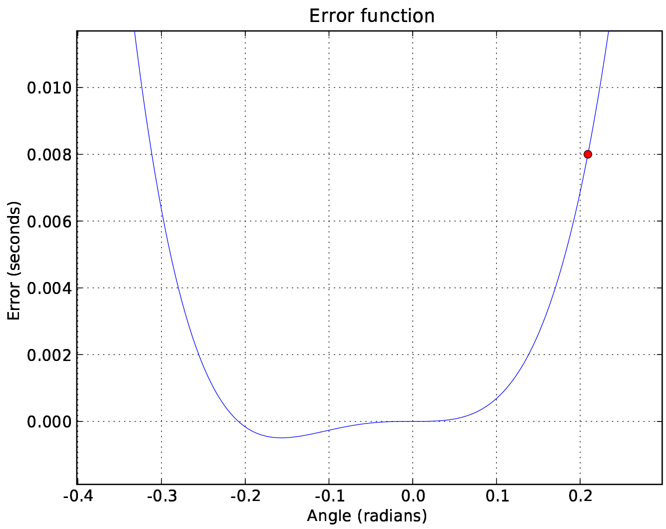

Fig. 5. Solution of the beam decomposition (the circle indicates the position of the solution)

Finally, we have :

$$\Delta T(\Delta\theta) = \frac{\Delta L_1}{V_1} + \frac{l' - l}{V_2} \quad (22)$$

If $|\Delta T(\Delta\theta)| < \epsilon$ then **J** can be the new point source for the outgoing beam.

4.3. *Solution to the PSB decomposition problem*

With the help of the previous results, we need, in order to solve the PSB decomposition, to determine the roots of an equation of the following type :

$$|\Delta T(\Delta\theta)| = \epsilon \quad (23)$$

As shown previously, this equation may have a solution or not, depending on the configuration. As classical methods have difficulties in finding the solutions in such a situation, we choose therefore to use a non conventional method to solve Eq. (5). It is based on winding number and has been used with success in other contexts such as in underwater acoustics for solving the characteristic equation of wave propagation in shallow water configurations.[13] Its main advantage is that it determines if there is or not a solution to the equation before solving it. This method is particularly useful in our case, since it avoids the consideration of all particular cases in which this equation has no solution. An example of the result of the solution of this equation is indicated in Fig. 5.

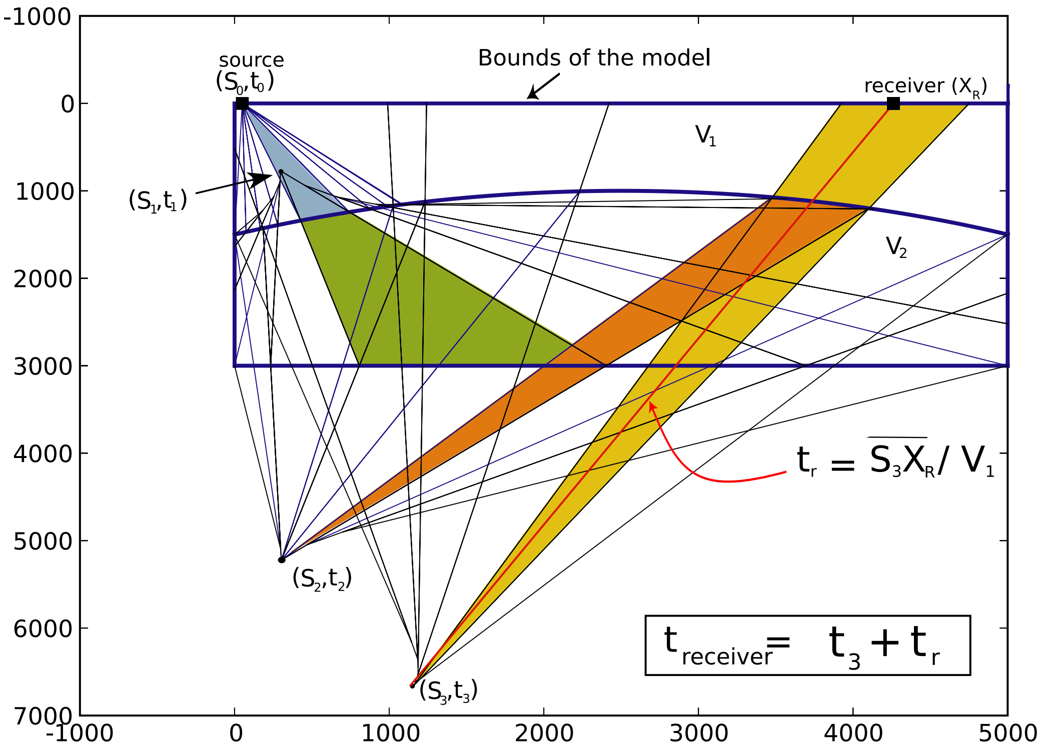

Fig. 6. PSB propagation in a multiple interface model

5. An illustrative example : the case of multiple interfaces

To complete the description of SBRT, we finish with the study of the propagation of PSB through the interfaces of the model. The main concern here is the criterion used to stop the propagation process and the way we calculate the traveltime between the source and a receiver. An example of the propagation of an individual PSB is presented in Fig. 6. For the sake of simplicity, we suppose that any of the PSB is divided, i.e. for each interface Eq. (23) has no solution. After the generation of an outgoing PSB, a control is made in order to determine the next interface which will be encountered. If the PSB reaches the bounds of the model then the propagation process is stopped. The propagation process is also stopped if the PSB reaches the place where the receivers are located. All the possible positions for the receivers are defined by a curve and two endpoints denoted, $\ell(\mathbf{A_1}, \mathbf{A_2})$. Otherwise, the interaction of the PSB with a new interface has to be considered. This is ilustrated in Fig. 6 where an initial PSB is successively transmitted, reflected and finally transmitted before reaching the receiver.

All generated beams are propagated until they are stopped, i.e. until they reach the bounds of the model or the receivers. Let *Sol* be the set of all PSB which reach the receivers :

$$Sol : \{B_i^R\}_{i=1,\cdots,N_R}$$

where N_R is the number of PSB which reach the receivers. Each PSB of this set can be written in the following form : $B_i^R : \{\mathbf{S_i^R}, t_i^R, \theta_l, \theta_r\}$.

The traveltime evaluation is performed in the following way. Given a receiver location $\mathbf{X_R}$, we look, among all B_i^R, for the ones which reach this position. Then, the traveltimes associated with this receivers are given by :

$$t_k = t_k^R + \frac{\overline{\mathbf{S_k^R X_R}}}{V_R} \quad k = 1, \cdots, K$$

where V_R is the velocity in the medium where the receiver lies and K the number of PSB which reach the receiver.

The bending problem which consists in finding the path which connects the source to a given receiver is easily solved with SBRT. This is not the case with classical methods, in a complex geometry context, because of the instability of the path perturbations (see Ref. 1 for more informations on the path determination problem). Moreover, if the position of the receivers is changed but stay within the limits of possible receiver positions, i.e. belongs to $\ell(\mathbf{A_1}, \mathbf{A_2})$, no additional calculus is necessary.

The trajectory followed by a ray can also be visualized by going back to the PSB which were created before attaining the receiver. An example of th.e rays which connect a source to an array of receivers is presented in Fig. 7. The model corresponds to a salt dome which is characterized by the presence of a low velocity layer embedded between two high velocity layers. This configuration can lead to a complex structure of ray trajectories leading to focusing and defocusing of the energy as it can be seen. This type of behaviour is not a problem for SBRT contrary to standard ray tracing methods. Note also that multiple reflection evaluation inside a layer which is still a difficulty for ray tracing algorithms[2] is easily implemented with SBRT.

6. Conclusion and perspectives

The goal of this paper was twofold : giving the basic principles of a new method for the fast evaluation of the traveltimes between a source and an array of receivers (called SBRT), and providing simple examples to illustrate its use. The originality of the method lies in the use of Information theory and Signal processing to simplify the model and the wave propagation process and to make in accordance the calculation with the resolution and the precision associated with the source signal. It results in a method which is optimal for the traveltime evaluation since it calculates only what is necessary, to get this information with a quality compatible with the characteristics of the source signal. This paper can be viewed as an introduction to the concepts used to build the new method SBRT for the study of wave propagation. SBRT can handle geometries which are much more complex than the example we provided. In addition to traveltimes, amplitudes can be evaluated with SBRT. Finally, it has to be noted that waves, propagating at the interfaces, such as head waves can also be included in SBRT. As these points are beyond the scope of this paper, they will be considered in future publications.

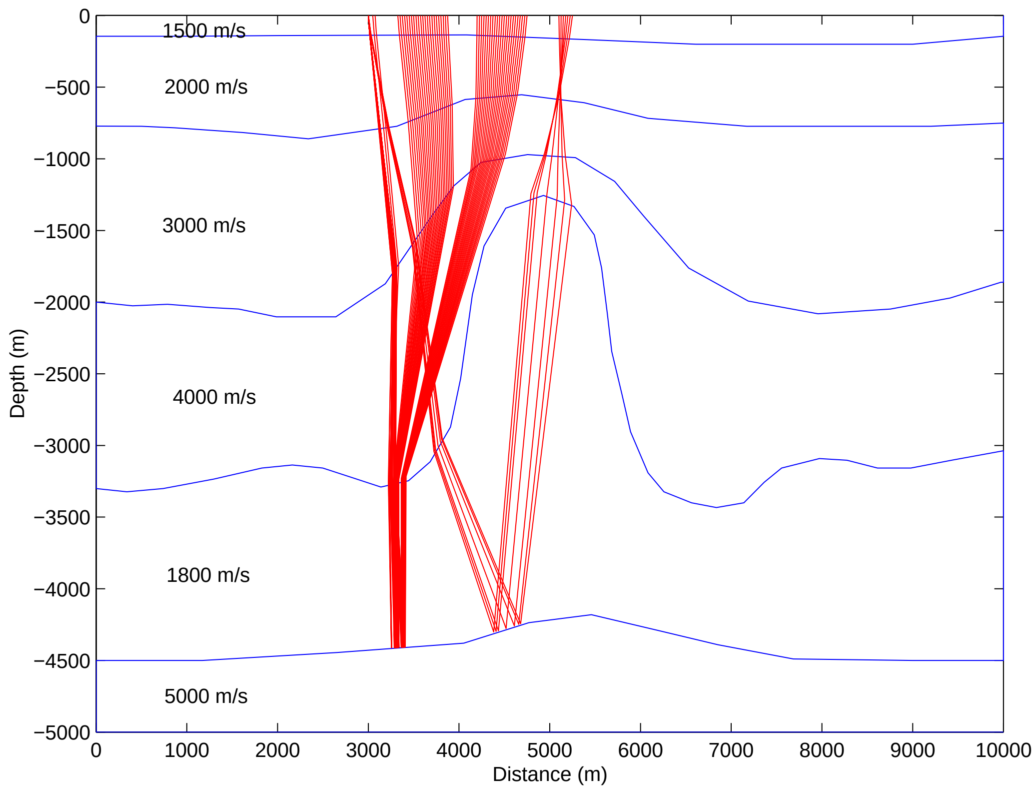

Fig. 7. Ray trajectories calculated with SBRT for a salt dome model

Acknowledgments

The authors wish to thank N. Favretto-Cristini for her careful reading of the manuscript and C. Revaux for the preparation of the figures.

References

1. V. Cerveny. *Seismic ray theory.* Cambridge University Press, 2001.
2. B. Engquist and O. Runborg. Computational high frequency wave propagation. *Acta Numerica*, 12:181–266, 2003.
3. E. De Bazelaire and J.F. Derain. Modelling by optical imagery. In *Proceedings of the SEG*, 1988.
4. F. Hoxha. *Fonctions de Green et migration de Kirchhoff par imagerie optique.* PhD thesis, Université de Pau et des Pays de l'Adour, 1992.
5. D. Gabor. Theory of communication. *I.E.E.E.*, 93(3):429–457, 1946.
6. C.E. Shannon. The mathematical theory of communication. *Bell System Technical Journal*, 12:181–266, 1949.
7. B. Boashash. *Time frequency signal analysis and processing : a comprehensive reference*, chapter 1, pages 12–19. Elsevier, 2003.
8. M. Born and E. Wolf. *Principles of Optics: Electromagnetic Theory of Propagation, Interference and Diffraction of Light.* Cambridge University Press, 7 edition, 13 October 1999.

9. J.-J. Lee and J.-Y. Hascoët. Smooth circular arc interpolation for planar free curves with tolerance control. *Proceedings of the I MECH E Part B, Journal of Engineering Manufacture*, 213(6):629–634, 1999.
10. H. Qiu, K. Cheng, and Y. Li. Optimal circular arc interpolation for NC tool path generation in curve contour manufacturing. *Computer-Aided Design*, 29:751–760, 1997.
11. L.A. Piegl and W. Tiller. Biarc approximation of NURBS curves. *Computer-Aided design*, 34:807–814, 2002.
12. H. Held and J. Eibl. Biarc approximation of polygons within asymmetric tolerance bands. *Computer-Aided Design*, pages 357–371, 2005.
13. P. Cristini. Fast and accurate method for the solution of the characteristic equation of shallow water in an isovelocity ocean. In J.S. Papadakis, editor, *Third European Conference on Underwater Acoustics*, pages 195–198, Heraklion, Crete, 1996.

Appendix

A. APPENDIX

In this appendix, we give some preliminary calculus needed for the solution of the PSB decomposition problem as shown in Fig. 4. We begin by considering the following vectors : $\overrightarrow{\mathbf{IC_0}}$, $\overrightarrow{\mathbf{IS_0}}$ and $\overrightarrow{\mathbf{T}}$ the tangent vector to the interface at the point **I**. Hence, we have :

$$\begin{aligned}\overrightarrow{\mathbf{IS_0}} &: \{X - R\cos\theta,\, Y - R\sin\theta\}\\ \overrightarrow{\mathbf{IC_0}} &: \{-R\cos\theta,\, -R\sin\theta\}\\ \overrightarrow{\mathbf{T}} &: \{-R\sin\theta,\, R\cos\theta\}\end{aligned}$$

where $X = X_s - X_c$ and $Y = Y_s - Y_c$

The scalar product of these vectors can be expressed in the following form :

$$\overrightarrow{\mathbf{IS_0}}.\overrightarrow{\mathbf{IC_0}} = R_1 L_1 \cos i_1 \quad \text{(A.1)}$$

$$\overrightarrow{\mathbf{IS_0}}.\overrightarrow{\mathbf{T}} = -R_1 L_1 \sin i_1 \quad \text{(A.2)}$$

where R_1 is the signed radius of the circle and L_1 is the signed curvature of the incoming wavefront.

Using the classical way of expressing the scalar product and Eqs. (A.1) and (A.2), we get :

$$X\cos\theta + Y\sin\theta = sgn(R_1)\,[R_1 - L_1\cos i_1] \quad \text{(A.3)}$$

$$X\sin\theta - Y\cos\theta = sgn(R_1)L_1\sin i_1 \quad \text{(A.4)}$$

In the same way, we get for the point $\mathbf{I}'$ of the interface corresponding to angle $\theta + \Delta\theta$:

$$X\cos(\theta+\Delta\theta) + Y\sin(\theta+\Delta\theta) = sgn(R_1)\left[R_1 - L_1'\cos i_1'\right] \quad \text{(A.5)}$$

$$X\sin(\theta+\Delta\theta) - Y\cos(\theta+\Delta\theta) = sgn(R_1)L_1'\sin i_1' \quad \text{(A.6)}$$

Then, from Eqs. (A.5) and (A.6), we can obtain an expression of $\cos i'_1$ and $\sin i'_1$ as a function of the angle of incidence i_1 and as a function of the angle variation $\Delta\theta$:

$$L'_1 \cos i'_1 = R_1 \left(1 - \cos \Delta\theta\right) + L_1 \cos \left(i_1 - \Delta\theta\right) \tag{A.7}$$

$$L'_1 \sin i'_1 = R_1 \sin \Delta\theta + L_1 \sin \left(i_1 - \Delta\theta\right) \tag{A.8}$$